

# Supplementary Information:

## Demonstration of an Ethane Spectrometer for Methane Source Identification

*Tara I. Yacovitch, Scott C. Herndon, Joseph R. Roscioli, Cody Floerchinger, Ryan M. McGovern, Michael Agnese, Gabrielle Pétron, Jonathan Kofler, Colm Sweeney, Anna Karion, Stephen Conley, Eric A. Kort, Lars Nähle, Marc Fischer, Lars Hildebrandt, Johannes Koeth, J. Barry McManus, David D. Nelson, Mark S. Zahniser, Charles E. Kolb*

Number of pages: 23

Number of figures: 14

# ***1. Supplemental Experimental Details***

## ***1.1. Integration into a mobile platform***

### ***1.1.1. Aerodyne Mobile Laboratory (AML)***

The Aerodyne Mobile Laboratory is a heavily modified step-van equipped with a flexible fleet of trace gas and particulate instruments. The full suite of instrumentation including the particulate phase measurement capabilities are described elsewhere.<sup>1</sup>

Numerous trace gas species are measured with the onboard tunable infrared laser absorption spectroscopy (TILDAS) based trace gas monitors. Two mini-chassis provide continuous measurements of 1) ethane and 2) nitrous oxide, water and carbon monoxide. A dual-laser instrument allows for the simultaneous measurement of methane, acetylene, water, and sulfur dioxide.

One Thermocube chiller per instrument is used to temperature stabilize the insulated optics boxes for the TILDAS instruments. Additional air conditioning has been added to the mobile lab. The ethane-mini Thermocube chiller is operated at 25 degrees C.

The ethane instrument mounting location varies depending on the required payload for any given campaign. Typically it is mounted using four inflatable vibration shock mounts to a custom built extruded aluminum (80-20) rack, but may also be mounted to the top of a second removable rack.

A TriScroll 600 Series Dry Scroll Vacuum Pump equipped with an isolation valve provides the flow through the Aerodyne Research Inc. mini and dual-QCL instruments, which are operated at in series at reduced pressure (30 – 70 Torr). Series operation means that the exhaust of the first TILDAS instrument is routed directly to the sample line of the second, and so on, so that the sample gas flows through each instrument in turn; the precise flow ordering varies depending on instrument installation location. Pressure control is accomplished with a MKS Pressure Controller Type 640 equipped with a 100 Torr head and powered by a MKS PR4000 digital power supply and display module. This unit is installed upstream of the TILDAS instruments and controls the downstream pressure.

Onboard wind measurements are taken by both rotary vane and sonic anemometers: a Vaisala Wind Sensor WM30 is mounted on the AML driver-side roof, and an Airmar LB150 or 200WX Ultrasonic WeatherStation is mounted near the inlet tip.

Multiple redundant GPS positioning systems are used on the AML. A Hemisphere V100 unit logs GPS position and static bearing, with backup GPS information available from a redundant Garmin 76 and the Airmar weather station.

In the AML, the TILDAS instruments stream mixing ratio data via RS232 to a data collecting computer. There, the RS232 feeds are logged to transient files, and sequentially loaded by a data

analysis computer. This is called the data exchange by file transfer protocol (DEFT), developed at Aerodyne Research, Inc.

### ***1.1.2. Mooney M20M-TLS aircraft***

The Mooney M20M-TLS aircraft is a heavily instrumented and modified research aircraft operated by Scientific Aviation. The aircraft platform has been described in detail elsewhere.<sup>2</sup>

The Ethane-Mini analyzer was installed in the cargo area, behind the pilot, with the Thermocube pump installed nearby. A 0.5 L refillable cylinder was used for carrying small amounts of zero gas for backgrounding. The instrument sampled through a filter from a dedicated ¼" Teflon inlet below the wing.

A Varian IDP-3 Dry Scroll Vacuum Pump provided the ~3 L/min flow through the ethane instrument. On this deployment, the ethane instrument used a dedicated inlet line; the methane inlet was a separate line routed out through the same under-wing sampling port. Pressure control was accomplished using a Swagelok solenoid valve controlled by the Ethane-Mini's TDL Wintel data acquisition software. The software uses a PID control algorithm based upon measured cell pressure. No optimization of the PID parameters was done prior to the flights, and no effect on reported ethane mixing ratio was observed for cell pressure fluctuations within 0.5 Torr. A factor of 10 improvement in pressure control should be possible with optimized control parameters.

Ethane mixing ratios are output from the instrument via an RS232 feed. In the aircraft, this RS232 feed is routed directly to a data acquisition laptop.

## ***1.2. Noise and Performance***

There are numerous possible reasons for an increase in noise when in motion, including: motion of interference fringes or other changes in optical baseline shape activated by accelerations, changes in the electromagnetic environment or simply vibrating cable connections. Several root causes of such effects are discussed below including alignment, vibrations/accelerations and temperature.

The noise performance of the instrument is typically worse if it becomes misaligned, and thus depends in part on the attention of the operator and care in setup. In the data examples shown in Figure 2 of the manuscript, the instrument had a high level of operator attention prior to the flight segments, including bi-weekly optical alignment. The ethane instrument was used in a more hands-off manner in the AML ground deployment, due to the multitude of other instruments running requiring attention. Thus, better alignment may be one reason for the improved noise in the aircraft vs AML.

Vibrations and accelerations may result in increased noise as they cause slight mechanical strain within the instrument (causing temporary misalignment) or otherwise activate optical fringes. The instrument was mounted in the AML with a vibration dampening rack, which we believe helps reduce its in-motion noise. In the aircraft, the instrument was only equipped with rubber corner bumpers, but not otherwise isolated. However, our impression is that vibrations and accelerations in the aircraft (excluding takeoff and landing) are more constant in nature

compared to the sporadic bumps, jolts and start-stops of the AML. The nature of the motion may thus compensate for the lack of vibrational isolation in the aircraft vs the AML.

Temperature stability of the instrument is also a factor in performance, since fluctuations can cause the optics to become slightly misaligned. This is most evident upon first turning on the instrument, as the laser and optical components come to their set temperature. Both the aircraft and the AML can undergo significant deviations from the instrument table temperature of 25 °C, especially in hot weather, or when taxiing (aircraft). Temperature regulation of the instrument optics box with the Thermocube chiller mediates these effects. We do not observe any significant temperature effects in the segments discussed within.

We have developed techniques for detailed analysis of the instrument spectra to inform us of the specific causes of increased noise in our instruments. Such analyses might inform on which specific optical fringe or electrical signal is contributing to the noise. These advanced techniques are specific to a given instrument at a given time, and are not generally applicable to the range of data presented within. Given the already high precision and signal-to-noise of these field results, such advanced analysis is beyond the scope of this work. In future work with mobile platforms, we plan to measure accelerations (including accelerations of the optical table itself) and perform spectral analysis in order to better understand and reduce excess in-motion noise.

## 2. Analysis Details

### 2.1. Water Correction

The ethane-Mini reports the wet molar mixing ratio, in ppb: this is equivalent to nano moles of ethane over moles of total sample. The instrument software includes a sophisticated algorithm allowing for the direct reporting of the dry mixing ratio by accounting for both dilution and pressure broadening effects, but this requires the presence of a water absorption line in the spectrum. Direct reporting of the dry mixing ratio is thus not possible for ethane in the current spectral region.

The dry mixing ratio can be largely recovered by correcting for the dilution effect of water. Several other instruments measure water in both deployments. The best water measurement, preferably one with 1-second data, can be used to correct mixing ratios for dilution. The dilution correction to the dry air mixing ratio is shown in equation 1, where  $C_s^{wet/dry}$  represents the molar mixing ratio of a species  $s$ , either wet or dry.

$$C_s^{dry} [ppb] = \frac{C_s^{wet}}{1 - \frac{n_{water}}{n_{tot}}} = \frac{C_s^{wet}}{1 - C_{water}^{wet}} = \frac{C_s^{wet} [ppb]}{1 - C_{water}^{wet} [\%] \cdot 10^{-2}} \quad 1$$

In plume analyses with the AML, the quantity of interest discussed in this paper, is the enhancement ratio of ethane to methane. The same dilution correction will thus be applied to the numerator (ethane) and the denominator (methane), cancelling out in the final ratio. This is not

the case, however, for ambient monitoring studies or studies where methane is reported in dry molar ppb. For reference consider an ambient ethane signal at 12 ppb. The dilution-only correction of the wet mixing ratio in a 2% water environment gives a dry mixing ratio of 12.24 ppb.

Dilution correction does not take into account the difference in pressure broadening of the ethane absorption line in humid air vs dry air. This means that the dry mixing ratio would appear to have a slight dependence on humidity. This effect is minor, up to around 30% of the dilution-only correction, and is less important at lower cell pressures. Water pressure broadening factors for the lines within the ethane spectrum at  $2997\text{ cm}^{-1}$  have not yet been experimentally verified.

In all of the AML data presented within, and all of the noise analysis segments, wet molar mixing ratios of methane and ethane were analyzed directly. For the determination of slopes using the Ethane-Mini and Methane-Dual TILDAS instruments, wet mixing ratios are preferred. The dilution correction in mixing ratios will cancel out, and the pressure broadening effect will partially cancel out. This is preferable to attempting a pressure broadening correction on one instrument and not the other; the humid-air pressure broadening will affect both ethane and methane mixing ratios in the same direction though not necessarily to the same degree. In the flight data, where dry methane mixing ratios were reported, the dry mixing ratio of ethane was computed after the fact using the water measurements from the onboard Picarro cavity ring-down spectroscopy (CRDS) instrument.<sup>3</sup> Any other ambient monitoring applications should also use dry ethane mixing ratios

## ***2.2. Dilution and Direct Overblow Calibrations***

The AML is equipped with a manifold of 5 critical flow orifices. During calibrations, the calibration gas is flown through this manifold and combined with the flow from a tank of ultra-zero air. Each flow is measured independently: the calibration gas flow through each orifice along with the flow from the zero air tank. The inlet of the AML is overblown with this diluted cal gas mix. Differing effective mixing ratios are obtained by varying the valving on the orifice manifold. 5 – 10 points are acquired for each calibration.

Dilution calibrations compliment the direct overblow calibrations since they can easily provide a flexible range of known concentrations using a single calibration tank. Figure S1 shows a dilution calibration of the 1000.0 ppb ethane standard. Data are measured immediately following a spectral background to eliminate any drift in the instrument zero. For this reason, the intercept is fixed at 0 in the fit. Calibration factors,  $C$ , are defined as

$$\text{Measured Mixing Ratio} = C \cdot \text{Standard Mixing Ratio} .$$

2

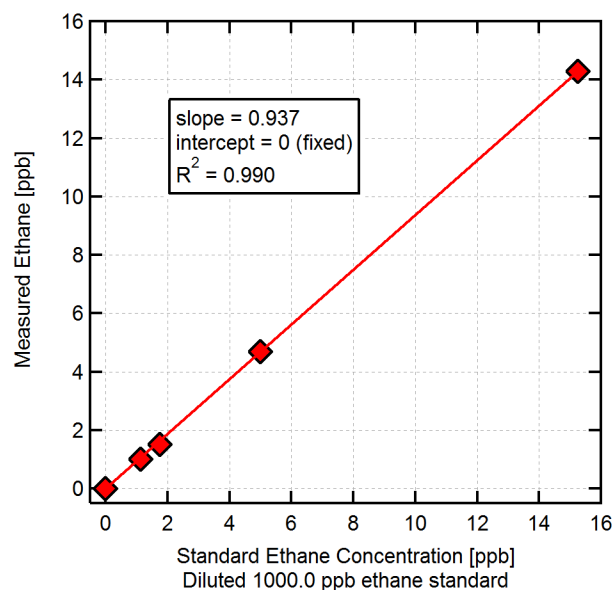


**Figure S1.** Dilution calibration of the 1000.0 ppb ethane standard on 2013/10/21

Table 1 summarizes the results of several calibrations over a period of time using three available standards. These results, and other measurements of these tanks by a second spectrometer, suggest that the 1060 ppb calibration tank is low, but until additional trusted standards can be obtained, we maintain an estimate of the instrument's systematic error, at ~6%.

**Table 1.** History of dilution and direct overblow calibrations of the ethane spectrometer

Date	Calibration Factor <sup>a</sup>	Method	Ethane Standard
2013/10/21	0.979	Direct overblow	17.57 ppb
2013/10/21	0.937	Dilution calibration	1000.0 ppb
2013/10/09	0.924	Dilution calibration	1000.0 ppb
2013/08/18	0.924	Direct overblow	1060 ppb
2013/08/18	0.987	Direct overblow	1000.0 ppb
2013/05/18	0.924	Direct overblow	1060 ppb
2013/05/18	0.980	Direct overblow	1000.0 ppb
2013/03/26	0.987	Direct overblow	1000.0 ppb
2012/10/04	0.927	Direct overblow	1060 ppb

<sup>a</sup>. Calibration factors, C, are defined in Equation 2

The methane calibration described in the manuscript text is shown in Figure S2. The procedure is the same as for the ethane calibration in Figure S1.

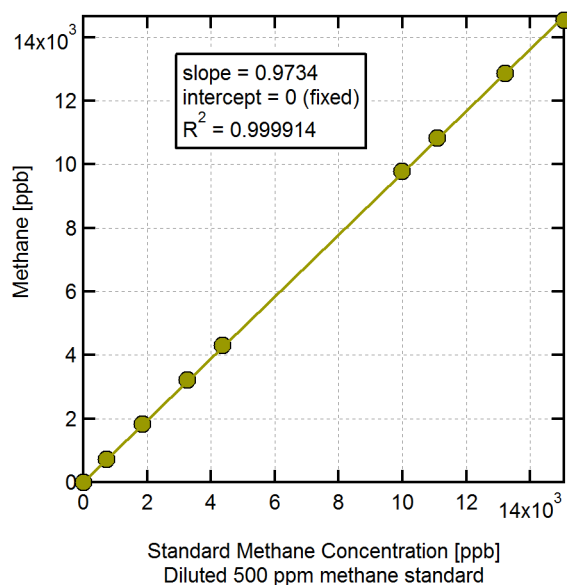


**Figure S2.** Dilution calibration of a 500 ppm methane standard on 2013/10/07

## 2.1. *Spectral Interferences*

No known interferences from species other than those included in the spectral fit are known to affect the ethane spectrum in the 2996 – 2998  $\text{cm}^{-1}$  spectral region. In the case of propane, the next-smallest alkane present in oil and gas emissions, Harrison *et al.* have performed experimental measurements of the 3  $\mu\text{m}$  band.<sup>4</sup> These show a broad shoulder over the short spectral range of interest, with a cross-section that is two orders of magnitude smaller than the ethane transitions<sup>5</sup> in question. Such a broad feature might, in extreme sampling concentrations, decrease the overall baseline light level in the ethane spectrum, decreasing the quality of the fit. However, more important to the ethane mixing ratio determination would be any changes in the overall baseline shape. Such baseline effects are accounted for with the higher-order polynomial fit used in determining the baseline in the ethane spectrum. Other larger hydrocarbons would be expected to have even broader absorptions with lower effective cross-sections.

## 2.2. *Estimate and treatment of non-single-mode character in laser*

The specification sheet provided by the manufacturer of the distributed feedback laser device shows the output intensity as a function of wavelength at a specific temperature and current. The test of the device used in this work (S/N891/4/-6) was characterized by a single mode emerging from a noise manifold at 3337 nm (2996.7  $\text{cm}^{-1}$ ).

Empirical tests of the laser mode purity were conducted by collecting spectra through a reference cell filled with sufficient ethane to saturate the absorption across the line center to nil. The difference between the light level at the ‘blackened’ peak and the off-period at the end of each scan quantifies the contribution of spurious light not at the ethane absorption wavelength. The result of such a test is shown in Figure S3. In this measurement, the  $\sim 3.8$  mV of separation between the line center at 2996.865  $\text{cm}^{-1}$  is less than 1% of the total, but would induce a 1% underestimate of the ethane concentration at the ranges relevant to this work.

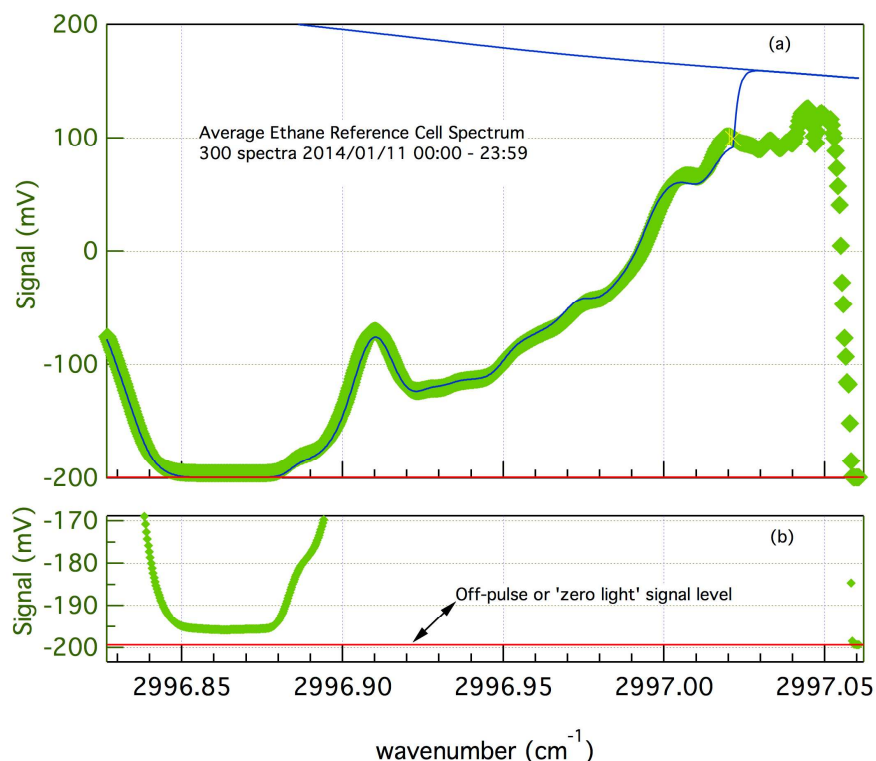


**Figure S3.** Assessment of light purity at ethane absorption center. The figure depicts the reference cell spectrum. In the upper panel, denoted (a), the full scale spectrum (green points) has been fit (blue line) using the spectral model described in the main article. In the lower panel, denoted (b), the same spectrum is depicted on an expanded scale. The red horizontal line is the detector signal level during the off-pulse (far right of the spectrum).

In practice, the appearance of stray light (at non-desired wavelengths such as that depicted above) over some portion the spectrum can cause 1) the bottom of a black (highly absorbing) spectrum to bottom out before the true 0 transmission level, as shown in Figure S3; 2) spectral artifacts due to strong absorbers of the non-desired wavelength appearing in the spectrum.

Observed reference cell spectra suggest that this ethane laser had periods of multi-mode stray light, including the observation of a small spurious absorption line appearing to the right of the small methane line in Figure 1 of the manuscript. This spurious line does not overlap with the ethane absorption line but could affect the fit of the small methane peak. A single and independently variable absorption line is added to the fit in order to prevent the spurious absorber, if present, from disrupting the fit of the methane line. Changing the driving electrical signals to the laser eliminates this effect when it occurs. The single-mode nature of the laser is monitored by 1) routine calibration and 2) frequent measurement of a black ethane spectrum through the use of a high concentration flip-in reference cell every 2 minutes.



### 2.3. Slopes

Ordinary least squares regression (OLS) is used to correlate the ethane and methane traces. For the final regression calculation, an orthogonal distance regression (ODR) was used. In most cases reported here, and for all cases where the quality of the fit was good, the difference in slope between regression types was insignificant, and did not change the reported values or uncertainties.

Uncertainties on the ethane/methane ratios are reported alongside the error at 95% confidence ( $\text{error} = t^{0.95} \cdot S_m$ ), calculated from the standard error of the intercept ( $S_m$  for slope  $m$ ). For this reason, the uncertainties shown in the data examples (Figure 3 of the manuscript, and Figure S4 to Figure S13) are tighter for examples with many data points. In cases where the quality of the fit is poor, only an upper limit to the ethane content is given ( $m + \text{error}$ ).

### 2.4. Keeling-like analysis

Characterization of methane sources can be done through methane isotope characterization. Such studies often display results as keeling plots, showing the isotope signature ( $\delta$ ) on the y-axis and the inverse concentration on the x-axis. If ethane is thought of as an “isotope” of methane, a Keeling-like plot<sup>6</sup> provides a familiar way of displaying the same information contained in the slope measurement. In practice, a correlation plot is produced prior to plotting the keeling plot, since it is convenient way of correcting for any small time offsets in the respective traces.

Equation 3 below defines  $\delta^{13}\text{C}$ , the carbon 13 isotope signature of methane. By convention, the sample’s methane isotope content is referenced to the Pee Dee Belemnite (PDB) standard with a known  $^{13}\text{C}/^{12}\text{C}$  ratio of 0.011237.  $^{13}\text{C}/^{12}\text{C}$  isotope ratios differ by only tiny amounts between samples; this convention emphasizes these small differences and expresses them on a unified scale. Here,  $^{13}\text{C}$  and  $^{12}\text{C}$  refer to concentrations of each methane isotope, and the final units are expressed in per-mil (‰).

$$\delta^{13}\text{C} = \left[ \frac{\left( \frac{^{13}\text{C}}{^{12}\text{C}} \right)_{\text{sample}} - \left( \frac{^{13}\text{C}}{^{12}\text{C}} \right)_{\text{PDB}}}{\left( \frac{^{13}\text{C}}{^{12}\text{C}} \right)_{\text{PDB}}} \right] \cdot 1000\text{‰} \quad 3$$

Equation 4 defines an analogous measure for the ethane content of a methane source. The concentration of ethane is  $C_2$ , the concentration of methane is  $C_1$  and the final units are in percentage. Here, no standard reference is used. The range of  $C_2/C_1$  encountered in the field is significantly greater than the range in  $^{13}\text{C}/^{12}\text{C}$ , eliminating the need for a scale that emphasizes small differences.

$$\delta C_2 = \left[ \left( \frac{C_2}{C_1} \right)_{sample} \right] \cdot 100 \% \quad 4$$

Analogously to traditional Keeling plots,<sup>6</sup> the ethane Keeling plot,  $\delta C_2$  vs  $1/C_1$ , can be fit to a straight line with slope  $q$ , and the intercept  $r$  corresponding to the source-specific  $\delta C_2$  (Equation 5).

$$\delta C_2 = q \frac{1}{C_1} + r \quad 5$$

Substituting in equation 4 and rearranging shows that the intercept of the ethane Keeling plot is equivalent to the slope of a correlation plot with formula  $C_2 = m \cdot C_1 + b$ .

$$C_2 = \frac{q}{100\%} + \frac{r}{100\%} C_1 \quad 6$$

$$m = \frac{r}{100\%} \quad 7$$

In the data examples shown within, keeling intercepts are reported alongside the error at 95% confidence (error =  $t^{0.95} \cdot S_r$ ), calculated from the standard error of the intercept ( $S_r$  for intercept  $r$ ). Ordinary least squares regression (OLS) is used in all keeling plots since it has been shown that both geometric mean regression and orthogonal distance regression can introduce biases in the retrieved  $\delta$ .<sup>7</sup>

In some cases, there are differences in the intercept of the Keeling plot and the slope of the correlation plot. These occur for cases where methane varies over only a very small range, a data limitation that is directly associated with uncertainty in  $\delta$ ,<sup>7</sup> and for cases where the quality of the linear regression is poor (low  $R^2$ ; large standard errors of the slope/intercept). Examples of such cases can be seen in Figure S6, and others. For cases where the error in the measurement exceeded the actual value of the retrieved  $\delta$ , only an upper or lower limit is given ( $r + \text{error}$  or  $r - \text{error}$ ).

### **3. Measurements of Known Sources**

Table 1 of the manuscript contains a number of experimentally measured ethane/methane ratios for methane sources of known type. The following sections contain additional source information, time series, and ethane/methane correlation and Keeling plots supporting these table entries.

### 3.1. *Municipal Landfill, Dallas Fort-Worth: < 0.0001 %*

A municipal landfill north of Dallas Fort-Worth was visited in March of 2013. Transects were performed downwind and large amplitude methane enhancements were observed. The large methane signal variation allows for the determination of a very tight upper limit to the possible ethane/methane enhancement ratio of < 0.0001%.

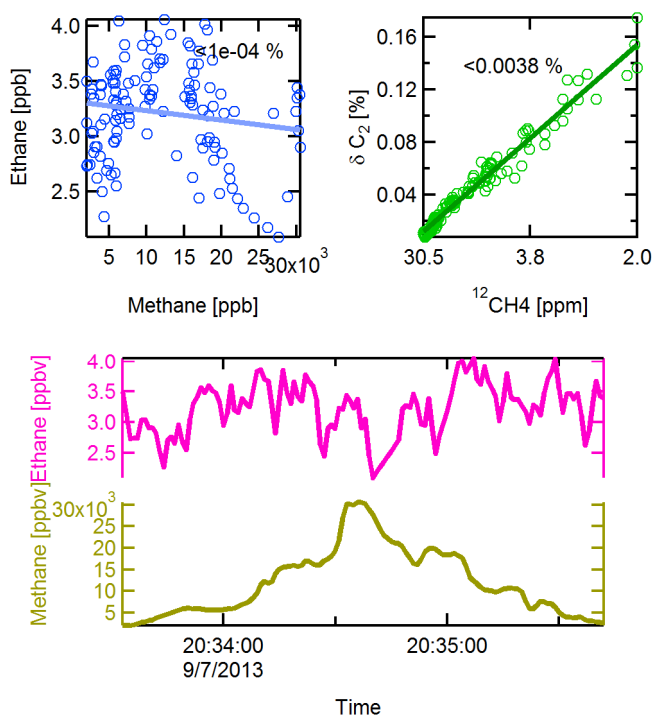


**Figure S4.** Municipal landfill plume. Mixing ratios for ethane (pink) and methane (gold) are shown below the slope (blue) and Keeling (green) analyses of the ethane/methane enhancement ratio.

### 3.2. Wastewater Treatment Facility, Dallas Fort-Worth: < 0.01 %

A wastewater treatment facility north of Dallas Fort-Worth was visited. Methane produced at this facility was measured along with co-emitted bacterial nitrous oxide ( $\text{N}_2\text{O}$ ). Wind measurements further confirm the source location and identity. There is no correlation between ethane and methane, and so only an upper limit to the enhancement ratio is given.

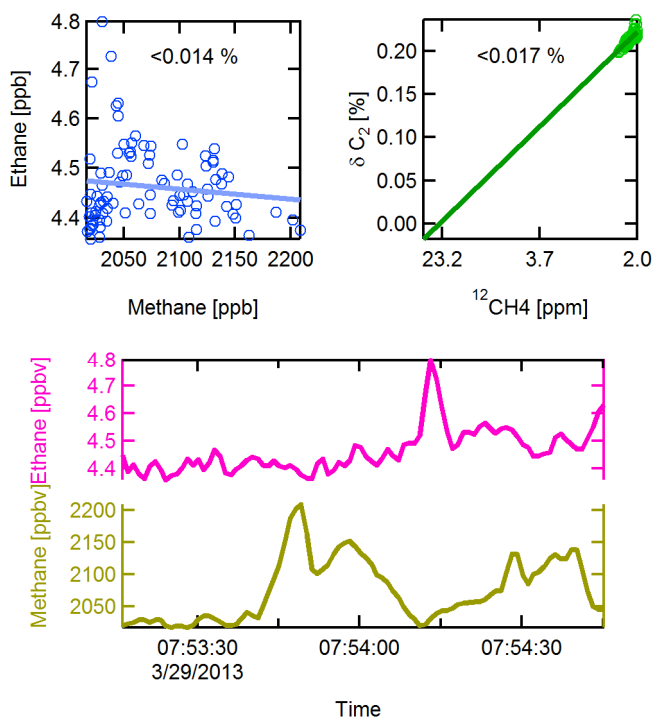


**Figure S5.** Wastewater treatment station plume. Mixing ratios for ethane (pink) and methane (gold) are shown below the slope (blue) and Keeling (green) analyses of the ethane/methane enhancement ratio.

### 3.3. Stagnant water, Houston area: < 0.05 %

A pool of stagnant water was repeatedly measured at Manvel-Croix Park, near Houston. This source was observed multiple times over the course of several days and under various wind conditions. One such observation is shown below. The relatively small methane enhancements do not allow for the determination of very tight upper limits to the ethane/methane enhancement ratio.

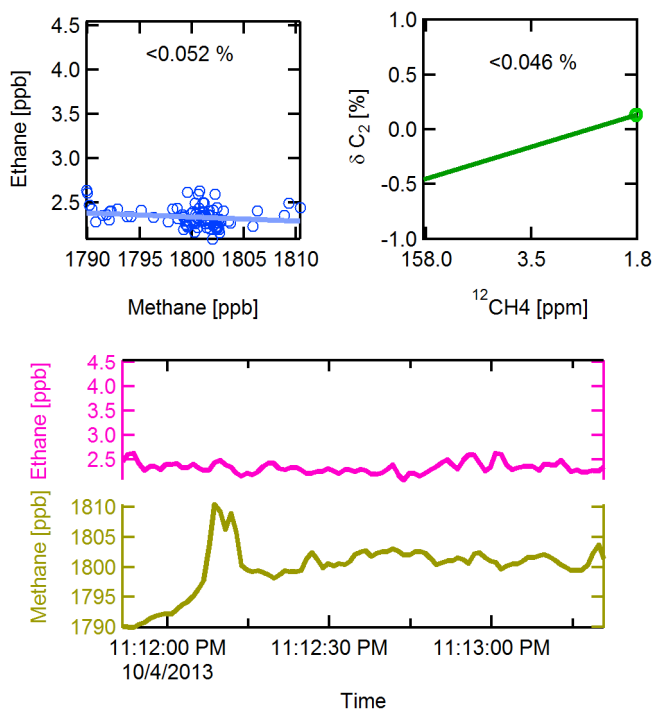


**Figure S6.** Stagnant water plume. Mixing ratios for ethane (pink) and methane (gold) are shown below the slope (blue) and Keeling (green) analyses of the ethane/methane enhancement ratio.

### 3.4. *Liquefied Natural Gas Tank Venting: 0.029 %*

Excess pressure is vented from an LNG tanker truck. The source of this LNG is from a western US state. This type of emission event is distinguished from other possible LNG events such as spilled LNG or emissions during tank filling or dispensing. A single plume is shown in Figure S7 below, though five replicate plumes were acquired, with an average ethane/methane enhancement ratio of  $0.029 \pm 0.001$  %. The large methane enhancements observed with this data allow for a precise determination of the low ethane content of this LNG plume.

Industry reports suggest that, similar to distribution-grade NG, LNG ethane content is determined by the heating content of the product.<sup>8</sup>

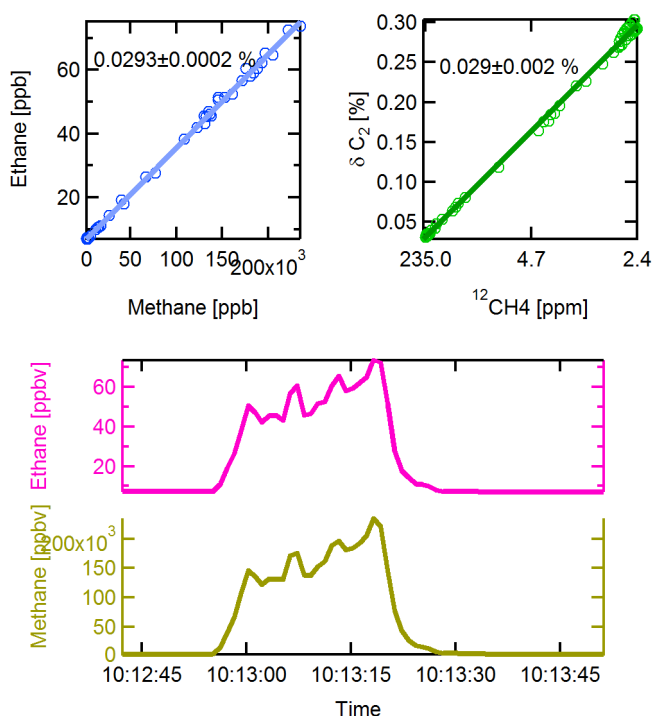


**Figure S7.** LNG tanker-truck venting plume. Mixing ratios for ethane (pink) and methane (gold) are shown below the slope (blue) and Keeling (green) analyses of the ethane/methane enhancement ratio.

### 3.5. City of Boston Gas Leaks, Boston University Rooftop: 1.8 – 2.3%

Five days of continuous measurements were performed on the rooftop of Boston University. A distribution of ethane/methane ratios was made by collecting all segments for which methane mixing ratios changed by  $> 200$  ppb. For each segment, an ethane/methane ratio was taken and added to the histogram shown below. The most common value for the ratio during these 5 days was 2.04 % ( $1\sigma = 0.25\%$ ). The full time series and correlation plot are also shown for this period.

Boston does not have significant oil and gas activity, beyond infrastructure for NG distribution. The limits for the expected ethane content of distribution-grade NG is restricted on a pipeline-by-pipeline basis by the same type of pipeline standards and pipeline agreements as for transmission-grade NG, i.e.  $< 15\%$ . For the Tennessee Gas pipeline, one of three serving the Boston area, pipeline agreements state a maximum ethane content of the gas of  $\sim 12\%$ .<sup>9</sup> Actual ethane content in the pipeline is significantly lower.

The EIA maintains records for the heat content of consumer natural gas on a state-by-state basis.<sup>10</sup> Massachusetts' natural gas heat content for 2012 was 1035 BTU/ft<sup>3</sup> (pure methane is 1012.3 BTU/ft<sup>3</sup>; ethane is 1773.7 BTU/ft<sup>3</sup>). A crude ethane/methane ratio of 3.07 % for Massachusetts natural gas can be estimated assuming the natural gas law and ignoring all other trace components of natural gas other than ethane and methane.

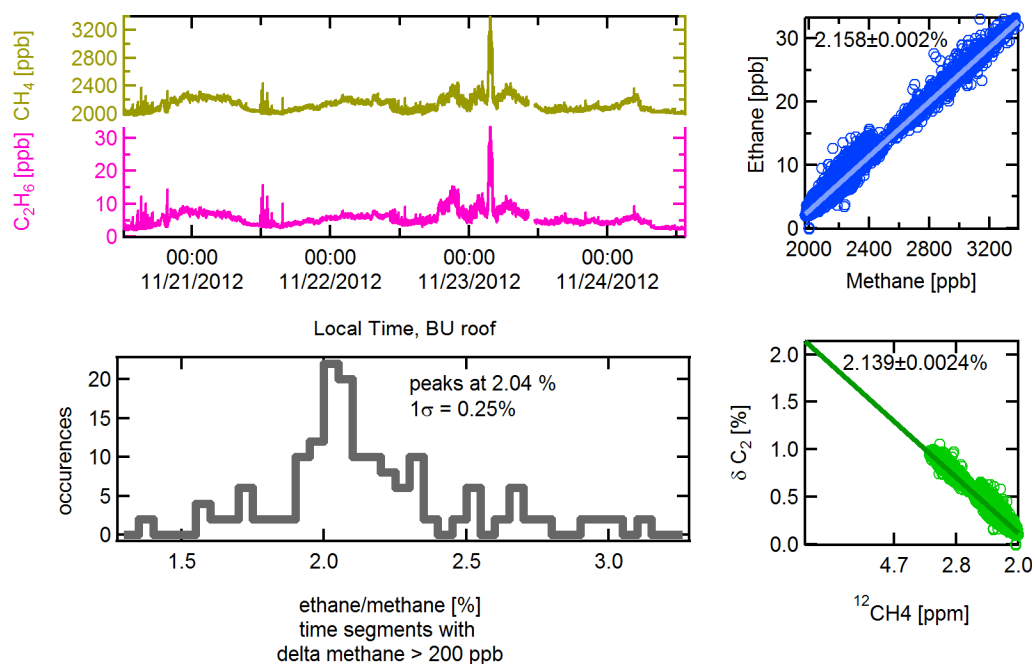


**Figure S8.** City of Boston gas leak plume. Mixing ratios for ethane (pink) and methane (gold) are shown along with the slope (blue) and Keeling (green) analyses of the ethane/methane enhancement ratio. A frequency of occurrence of any given ratio is also shown.

### 3.6. Compressor Station, north-eastern US: 2.20 %

This data was acquired downwind of a compressor station in the north-eastern US. This facility collects dry gas from wells in the region. Wind measurements indicated the facility upwind and an on-site operator identified and described the facility and was further able to confirm that the observed ethane/methane enhancement ratio agreed within ~10% of the ethane/methane ratios produced by the dry gas wells in the region.

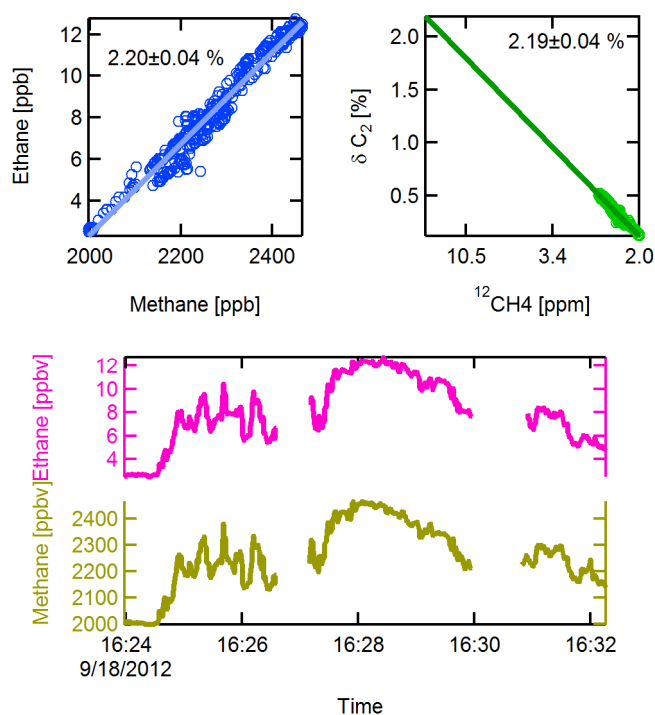


**Figure S9.** Compressor station plume. Mixing ratios for ethane (pink) and methane (gold) are shown below the slope (blue) and Keeling (green) analyses of the ethane/methane enhancement ratio.



### 3.7. 14 Compressor Stations: 1.0 – 3.5 %

During the EDF Transmission and Storage study,<sup>11</sup> numerous compressor stations were visited by the AML. These stations were geographically clustered and cannot be considered a representative sample of compressor stations across the US. Ethane/methane enhancement ratios for the methane emissions from each site were measured as in other examples.

Strict contracts and agreements on the allowed ethane content in pipeline gas determines the maximum allowed ethane content in the transmission system,<sup>12</sup> around <15 %. For 14 of the visited compressor stations, operator data was available on the gas composition of the natural gas at that station or at neighboring stations along the same pipeline. This operator data consists of in-line gas chromatography analysis. These gas analysis values are consistent with AML measured values, with ethane/methane ratios of 0.9 – 4.5 %, compared to measured values of 1.0 – 3.5 %. The measured values are averages of several replicate plume intercepts and are shown with error bars at 95% confidence levels.

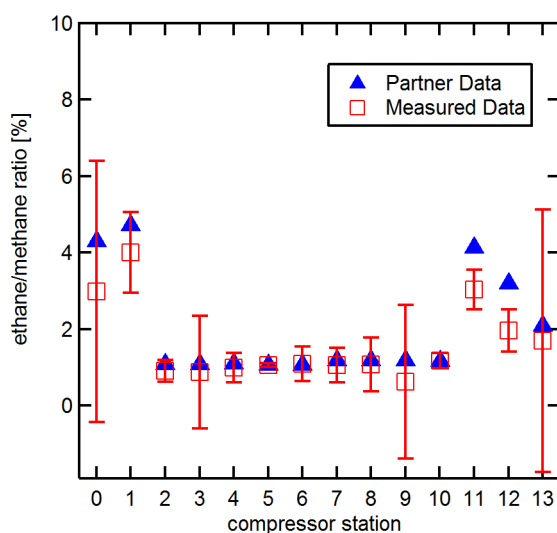


**Figure S10.** Operator data on the ethane content of compressor station pipeline gas is shown in blue. AML measured ethane/methane ratios with error bars reported at 95% confidence levels are shown in red.

### 3.8. Well Field, Wellsboro PA: 2.38 %

The AML was stationed overnight in Wellsboro, PA during the time period of the Production Study.<sup>13</sup> Overnight wind was out of the WSW, following the path of the surrounding valley. The average ethane/methane ratio observed was 2.38%, though a short duration event with a ratio of 6% occurs partway through the evening. This region has a high density of well sites producing sales-ready “dry” gas.

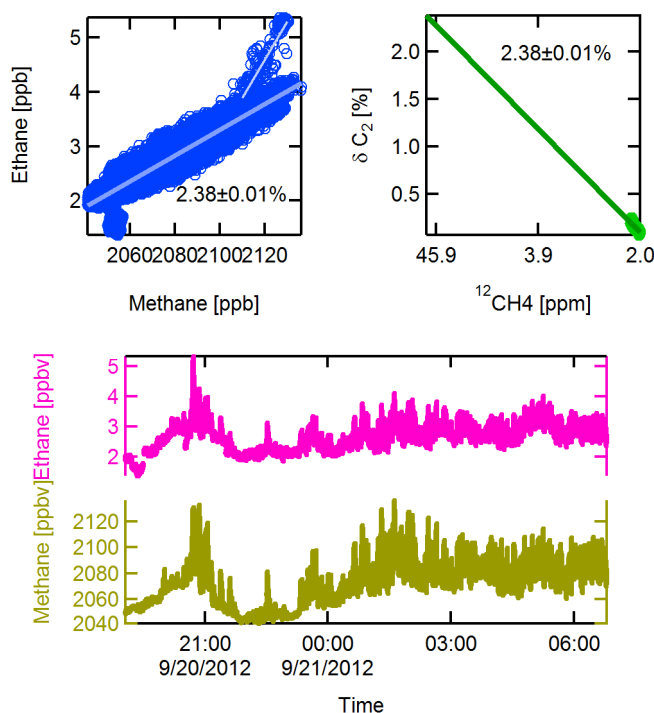


**Figure S11.** Dry gas field plume. Mixing ratios for ethane (pink) and methane (gold) are shown below the slope (blue) and Keeling (green) analyses of the ethane/methane enhancement ratio.

### 3.9. Gas Well, western US: 10.1%

This is a plume downwind of a small well pad in a wet gas region of the central US. This plume was measured next to the plant in Figure S13. An on-site operator was present and was able to confirm the equipment description.

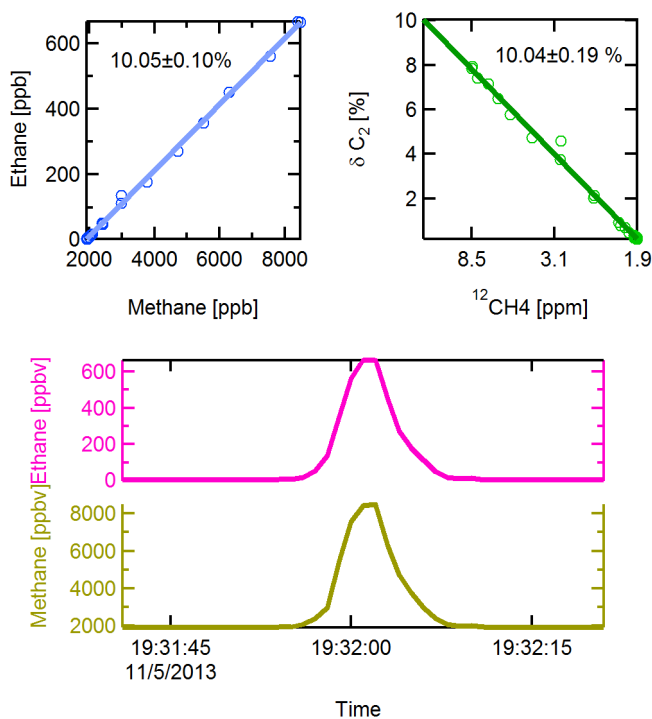


**Figure S12.** Gas well. Mixing ratios for ethane (pink) and methane (gold) are shown below the slope (blue) and Keeling (green) analyses of the ethane/methane enhancement ratio.

### 3.10. NG Processing Plant/Fractionator, western US: 45 %

Methane emissions were measured during a visit of the AML to a natural gas processing plant in a wet-gas region, western US. Natural gas liquids are separated into their various components for sale. This facility neighbored the wet gas well, shown in Figure S12 above. Equipment was described by on-site operator as a liquids processing plant.

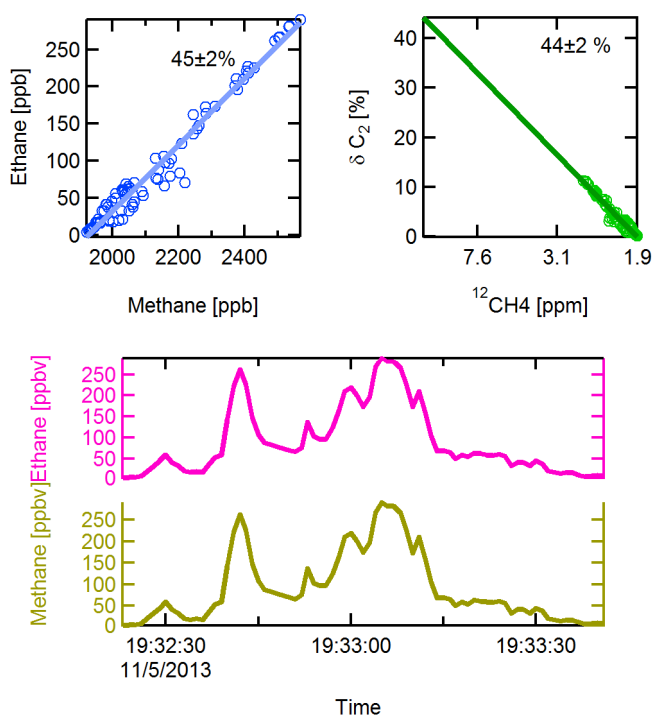


**Figure S13.** Liquids processing plume. Mixing ratios for ethane (pink) and methane (gold) are shown below the slope (blue) and Keeling (green) analyses of the ethane/methane enhancement ratio.

### 3.11. Chemical Plant Feedstock, Houston TX: ∞ %

This is a plume that was acquired on the FM1942 road in Mont Belvieu, near Houston, TX (29.507 N, 94.94 W). Mont Belvieu contains a high density of facilities that produce ethene. A chemical precursor for ethene is ethane and can be transported in the hazardous liquid pipeline system. Maps of the liquid pipeline system indicate a high density of lines connecting Mont Belvieu facilities to liquids processing plants in other regions.<sup>14</sup> The mobile laboratory performed two transects of the area and noted that the mixing ratio of ethane was greatest downwind of a point where the pipeline system crossed FM1942.

There is no correlation between ethane and methane in this plume ( $R^2$  of the fits are  $\sim 0.03$ ), yielding slopes around 132 %, but lower limits to the ethane/methane enhancement ratios are calculated by two methods: plotting ethane vs methane and plotting methane vs ethane. The ODR type of linear regression fails for the ethane vs methane plot (blue); the simpler OLS fit is shown instead.

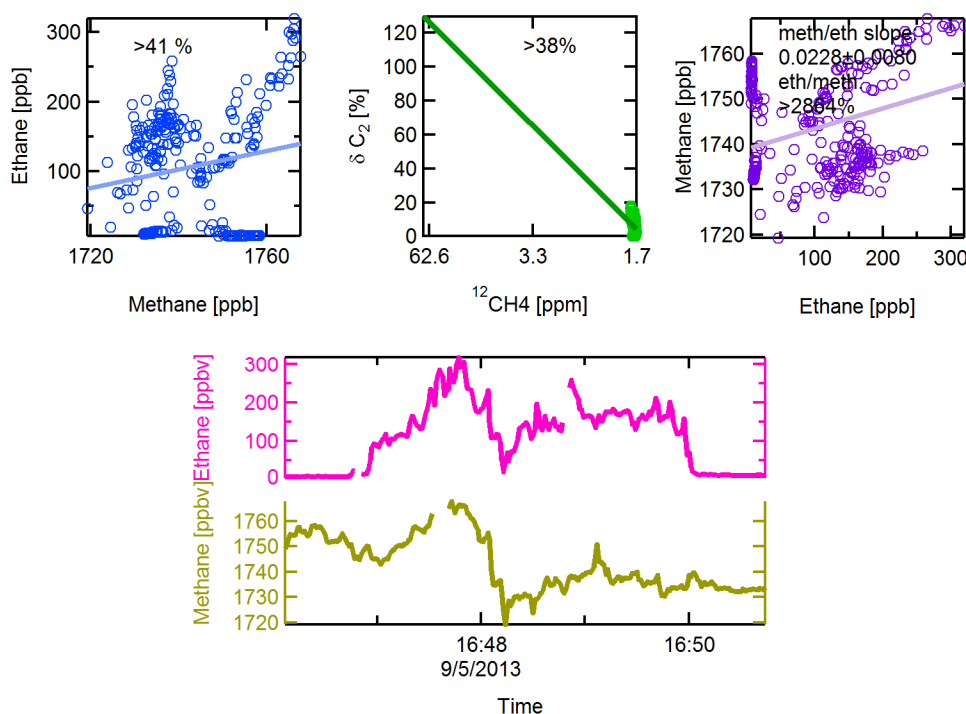


**Figure S14.** Chemical plant feedstock plume. Mixing ratios for ethane (pink) and methane (gold) are shown below the slope (blue) and Keeling (green) analyses of the ethane/methane enhancement ratio.

## 4. References.

- (1) Kolb, C. E.; Herndon, S. C.; McManus, B.; Shorter, J. H.; Zahniser, M. S.; Nelson, D. D.; Jayne, J. T.; Canagaratna, M. R.; Worsnop, D. R. Mobile laboratory with rapid response instruments for real-time measurements of urban and regional trace gas and particulate distributions and emission source characteristics. *Environ. Sci. Technol.* **2004**, *38*, 5694.
- (2) Karion, A.; Sweeney, C.; Pétron, G.; Frost, G.; Michael Hardesty, R.; Kofler, J.; Miller, B. R.; Newberger, T.; Wolter, S.; Banta, R.; Brewer, A.; Dlugokencky, E.; Lang, P.; Montzka, S. A.; Schnell, R.; Tans, P.; Trainer, M.; Zamora, R.; Conley, S. Methane emissions estimate from airborne measurements over a western United States natural gas field. *Geophys. Res. Lett.* **2013**, *40*, 4393; DOI 10.1002/grl.50811.
- (3) Crosson, E. R. A cavity ring-down analyzer for measuring atmospheric levels of methane, carbon dioxide, and water vapor. *Appl. Phys. B.* **2008**, *92*, 403; DOI 10.1007/s00340-008-3135-y.
- (4) Harrison, J. J.; Bernath, P. F. Infrared absorption cross sections for propane (C<sub>3</sub>H<sub>8</sub>) in the 3  $\mu$ m region. *J. Quant. Spectrosc. Radiat. Transfer.* **2010**, *111*, 1282; DOI <http://dx.doi.org/10.1016/j.jqsrt.2009.11.027>.
- (5) Harrison, J. J.; Allen, N. D. C.; Bernath, P. F. Infrared absorption cross sections for ethane (C<sub>2</sub>H<sub>6</sub>) in the 3  $\mu$ m region. *J. Quant. Spectrosc. Radiat. Transfer.* **2010**, *111*, 357; DOI 10.1016/j.jqsrt.2009.09.010.
- (6) Keeling, C. D. The concentration and isotopic abundances of carbon dioxide in the atmosphere. *Tellus.* **1960**, *12*, 200; DOI 10.1111/j.2153-3490.1960.tb01300.x.
- (7) Zobitz, J. M.; Keener, J. P.; Schnyder, H.; Bowling, D. R. Sensitivity analysis and quantification of uncertainty for isotopic mixing relationships in carbon cycle research. *Agric. For. Meteorol.* **2006**, *136*, 56; DOI 10.1016/j.agrformet.2006.01.003.
- (8) Coyle, D.; de la Vega, F. F.; Durr, C. *Natural gas specification challenges in the LNG industry*; Paper PS4-7; KBR: Houston, TX, 2007. <http://www.kbr.com/Newsroom/Publications/technical-papers/Natural-Gas-Specification-Challenges-in-the-LNG-Industry.pdf> (accessed 02/14/2014).
- (9) *FERC NGA gas tariff, sixth revised volume no. 1*; Tennessee Gas Pipeline Company L.L.C.: Houston, TX, 2011. <http://tebb.elpaso.com/ebbmastertpage/Tariff/OrgChart.aspx?code=TGP&status=GQ&pdf tag=gtcq>
- (10) *Heat content of natural gas consumed*; U.S. Energy Information Administration: Washington, D.C., 2012. [http://www.eia.gov/dnav/ng/ng\\_cons\\_heat\\_a\\_EPG0\\_VGTH\\_btucf\\_a.htm](http://www.eia.gov/dnav/ng/ng_cons_heat_a_EPG0_VGTH_btucf_a.htm)
- (11) Gathering facts to find climate solutions, 2014. Environmental Defense Fund Website. <http://www.edf.org/climate/methane-studies> (accessed 01/31/2014).
- (12) AES ocean express LLC v. Florida gas transmission company and Southern Natural Gas Company. *121 FERC 61.267*, Docket No. RP04-249-006, 2007; Federal Energy Regulatory Commission, Opinion No. 495-A Order on Rehearing.
- (13) Allen, D. T.; Torres, V. M.; Thomas, J.; Sullivan, D. W.; Harrison, M.; Hendler, A.; Herndon, S. C.; Kolb, C. E.; Fraser, M. P.; Hill, A. D.; Lamb, B. K.; Miskimins, J.;

- Sawyer, R. F.; Seinfeld, J. H. Measurements of methane emissions at natural gas production sites in the United States. *Proc. Natl. Acad. Sci. U. S. A.* **2013**, *110*, 17768; DOI 10.1073/pnas.1304880110.
- (14) *Pipeline information management mapping application*; Pipeline and Hazardous Materials Safety Administration, U.S. Department of Transportation: Washington, DC, 2007. <https://www.npms.phmsa.dot.gov/>